A Family of IIR Two-Band Orthonormal QMF Filter Banks

Sanja Damjanovic[1], Ljiljana Milic[2]

Abstract: The design and characteristics of orthonormal two-band QMF filter banks, with perfect reconstruction and linear phase properties, are considered in this paper. The analysis and synthesis filter banks are implemented using allpass filters. Filters in the synthesis bank are anticausal and unstable filters and the block processing technique and an appropriate causal filter are applied for their real time application. The generated filter banks characteristics and the finite block length influence of the block processing technique applied for anticausal filtering are illustrated for a rectangular input signal case. The corresponding wavelet and scaling functions, generated after five iterations of the analysis bank in a lowpass branch, are shown.

Keywords: IIR, QMF, Filter bank, Block processing technique, Wavelets.

1 Introduction

In this paper, two-band paraunitary filter banks, which, when iterated, generate orthonormal wavelet bases are considered. Orthonormal filter banks can be realized using finite impulse response (FIR) or infinite impulse response (IIR) filters. The case of FIR filters has been examined in detail, while IIR filter banks have been less studied [1, 2]. It is known that IIR filters composed of two real allpass filters can be implemented with low complexity structures that are robust to finite precision error [3]. The main advantage of IIR filter banks is good frequency selectivity. Linear phase and orthonormality are not mutually exclusive properties for IIR filter banks, as they are in FIR case. To accomplish the orthonormality property, the impulse responses of the synthesis bank filters must be the time-reversed versions of the analysis filters. In the case of an FIR filter bank, that is achieved simply by filter coefficients time-inversion. If the IIR analysis filter bank uses causal filters, then the synthesis has anticausal filters.

In this paper, we use the algorithm proposed in [4, 5] and develop a design method for IIR complementary half-band filter pairs. The z-plane poles of designed half-band filters are placed on the imaginary axis. We use the block processing technique [6, 7] for the anticausal implementation of the synthesis part of the analysis bank. The results of

---

[1] Mihailo Pupin Institute, Volgina 15, 11000 Belgrade,
  Serbia&Montenegro, E-mail: sanja@kondor.imp.bg.ac.yu
[2] School of Electrical Engineering, Kralja Aleksandra 73, 11000 Belgrade,
  Serbia&Montenegro, E-mail: milic@kondor.imp.bg.ac.yu

the analysis of the implemented QMF bank are given in the paper. Finally, the appropriate scaling and wavelet functions are generated.

2   Filter Design

Let $H_0(z)$ and $H_1(z)$ denote the transfer functions of the lowpass and highpass filter of the analysis part of the two-channel quadrature-mirror filter (QMF) bank, and let $G_0(z)$ and $G_1(z)$ denote the transfer functions of the lowpass and highpass filter of the synthesis part. By choosing transfer functions to satisfy conditions [4]:

$$H_1(z) = H_0(-z),\tag{1}$$

$$G_0(z) = H_0(z^{-1}) \text{ and}\tag{2}$$

$$G_1(z) = H_1(z^{-1}) = H_0(-z^{-1}),\tag{3}$$

the filter bank has the perfect reconstruction and orthonormal properties. If $H_0(z)$ and $H_1(z)$ are based on the parallel connection of two real allpass filters, $A_0(z)$ and $A_1(z)$, their transfer functions are

$$H_0(z) = \frac{1}{2}\left(A_0(z^2) + z^{-1}A_1(z^2)\right) \text{ and}\tag{4}$$

$$H_1(z) = \frac{1}{2}\left(A_0(z^2) - z^{-1}A_1(z^2)\right).\tag{5}$$

It can be seen that the magnitude responses of $H_0(z)$ and $H_1(z)$ satisfy the following power-complementary relation,

$$\left|H_0(e^{j\omega})\right|^2 + \left|H_1(e^{j\omega})\right|^2 = 1,\tag{6}$$

which means that the design of only one filter, $H_0(z)$, needs to be considered.

The bases vectors of orthonormal wavelet transformation are obtained from the iteration of this filter bank on its lowpass branch, with the additional "flatness" constraint that the lowpass filter should have K zeros at half the sampling frequency [1]. Iteration of filter bank generates equivalent band-pass filters of the form

$$\Psi^i(z) = H_0(z)H_0(z^2)\cdots H_0(z^{2^{i-2}})H_1(z^{2^{i-1}}).\tag{7}$$

Letting $i \to \infty$ gives the "mother wavelet" $\psi(t)$:

$$\psi(t) = \lim_{i \to \infty} \psi^i_{\left\lfloor 2^i t \right\rfloor},\tag{8}$$

where ψ^i_n is the impulse response of $\psi^i(z)$.

The filter bank is never iterated to infinity in practice, so a desirable property is the ability of the waveform of ψ_n^i to vary smoothly in time n. This can be imposed by requiring that the limit function $\psi(t)$ exists and is regular i.e. continious, possibly with several continuous derivatives. Regularity is usually qualified by measuring the "regularity order", which can be defined as the number of times $\psi(t)$ is continuously differentiable. The simplest regularity condition for filter design is flatness constraint on the magnitude response $|H_0(z)|$ at the Nyquist frequency ($\omega = \pi$). The K th-order flatness is obtained if $H_0(z)$ contains K zeroes located at $z = -1$,

$$\left.\frac{\partial^k \left|H_0(e^{j\omega})\right|}{\partial \omega^k}\right|_{\omega=\pi} = 0 \, , \ (k = 0,1,...,K-1) \, . \tag{9}$$

For a given filter order, regularity and frequency selectivity contradict each other, so the design of $H_0(z)$ that has the best possible frequency selectivity for a given flatness condition is important.

3 Algorithm Description

The design of IIR filter $H_0(z)$ using a parallel sum of two real allpass filters is based on an eigenvalue problem by using the Remez exchange algorithm [5]. From equation (4), it yields

$$H_0(z) = \frac{1}{2} A_0(z^2)\left(1 + z^{-1}U(z^2)\right), \tag{10}$$

where $U(z)$, a Nth-order real allpass filter, is defined as

$$U(z) = \frac{A_1(z)}{A_0(z)} = z^{-N} \frac{\displaystyle\sum_{n=0}^{N} a_n z^n}{\displaystyle\sum_{n=0}^{N} a_n z^{-n}}, \tag{11}$$

where the filter coefficients a_n are real, and $a_0 = 1$. The phase response $\vartheta(\omega)$ of $z^{-1}U(z^2)$ is

$$\vartheta(\omega) = 2\tan^{-1} \frac{\displaystyle\sum_{n=0}^{N} a_n \sin\theta_n(\omega)}{\displaystyle\sum_{n=0}^{N} a_n \cos\theta_n(\omega)}, \tag{12}$$

where $\theta_n(\omega) = (2n - N - \frac{1}{2})\omega$. The amplitude response of $H_0(z)$ is given by

$$a(H_0(e^{j\omega})) = \cos\frac{\vartheta(\omega_i)}{2} = \frac{\displaystyle\sum_{n=0}^{N} a_n \cos\theta_n(\omega)}{\sqrt{\left(\displaystyle\sum_{n=0}^{N} a_n \sin\theta_n(\omega)\right)^2 + \left(\displaystyle\sum_{n=0}^{N} a_n \cos\theta_n(\omega)\right)^2}}. \quad (13)$$

To meet the flatness condition in equation (9), the following relation must be satisfied

$$\sum_{n=0}^{N} a_n\left(2n - N - \frac{1}{2}\right)^{2m-1} = 0, \quad m = 1, 2, ..., M, \quad (14)$$

where $K = 2M + 1$ is odd, and M is integer and $0 \leq M \leq N$. When $M = N$, $H_0(z)$ becomes a maximally flat filter, and the solution can be obtained by solving only the linear equation (14) for $a_0 = 1$. When $0 \leq M < N$, the aim is to achieve an equiripple magnitude response by using remain degree of freedom. It can be concluded from equations (1) and (6) that only stopband response needs to be approximated. First, $N - M + 1$ extreme frequencies ω_i in the stopband $[\omega_s, \pi]$ are selected as follows,

$$\omega_s = \omega_0 < \omega_1 < ... < \omega_{(N-M)} < \pi. \quad (15)$$

By using the Remez exchange algorithm and the equation (13), the following can be written

$$a(H_0(e^{j\omega_i})) = \cos\frac{\vartheta(\omega_i)}{2} = (-1)^i \delta_m \text{ and} \quad (16)$$

$$\frac{\displaystyle\sum_{n=0}^{N} a_n \cos\theta_n(\omega_i)}{\displaystyle\sum_{n=0}^{N} a_n \sin\theta_n(\omega_i)} = \coth\left(\cos^{-1}(-1)^i \delta_m\right) = (-1)^i \delta, \quad (17)$$

where $\delta_m \, (>0)$ is amplitude error, $\delta = \delta_m / \sqrt{1 - \delta_m^2}$, and the denominator polynomial must be different from zero.

Equations (14) and (17) can be rewritten in a matrix form as

$$PA = \delta QA, \quad (18)$$

where $A = [a_0, a_1, ..., a_N]^T$, and the matrices P and Q are

$$P = \begin{bmatrix} P_1 \\ P_2 \end{bmatrix},$$

$$P_{1ij} = \left(2i - N - \frac{1}{2}\right)^{2(j+1)-1} , \ i = 0,1,...,N , \ j = 0,1,...,M-1 ,$$

$$P_{2ij} = \cos\theta_i(\omega_j) , \ i = 0,1,...,N , \ j = 0,...,N-M , \tag{19}$$

$$Q = \begin{bmatrix} Q_{N+1\times M} \\ Q_2 \end{bmatrix} \text{ and }$$

$$Q_{2ij} = (-1)^j \sin\theta_i(\omega_j) , \ i = 0,1,...,N , \ j = 0,...,N-M . \tag{20}$$

The set of filter coefficients can be get by solving the generalized eigenvalue problem (18), computing the absolute minimum eigenvalue δ. The optimal solution is obtained after several iterations. Once the optimal filter coefficients are obtained, the poles of $U(z)$ inside the unit circle are assigned to $A_1(z)$ as its poles and the poles outside the unit circle are assigned to $A_0(z)$ as its zeros to get causal and stable $H_0(z)$.

4   Real-Time Implementation of Orthonormal Filter Bank

A computationally efficient polyphase realization of two-channel IIR bank is depicted in Figure 1 [3]. In the synthesis bank filters polyphase components are anticausal and unstable filters. The causal implementation of the anticausal filter is based on the corresponding causal filter and the block processing technique [6,7]. The block processing technique is a direct procedure for the design with the smallest length of the time-reversed sequence and with a small processing delay and can be used for the processing of the infinite length sequences or very long finite input sequences. Figure 2 ilustrates this procedure for the polyphase filter $A_0(z^{-1})$ of the analysis bank. The infinite length input sequence is divided into L-length sequences, and each sequence is filtered separately as follows:

The input L-length sequence is stored in a last-in first-out (LIFO) register:

1) The time-reversed sequence is filtered using filter $A_0(z)$, yielding $2L$-length output sequence;

2) The sum of the last L output samples and the first L output samples of the previous sequence (delayed $2L$ samples) is the new sequence $f[n]$; and

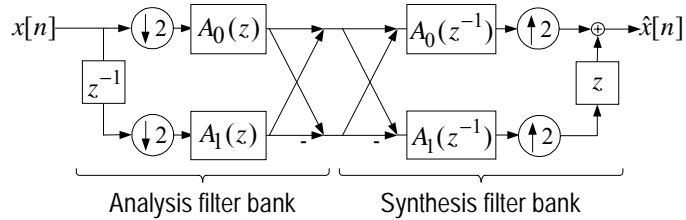3) The L-length sequence of $f[n]$ is time reversed using the LIFO register.

49

Fig. 1 – *Computationally efficient polyphase realization of two-channel magnitude-preserving IIR QMF bank.*
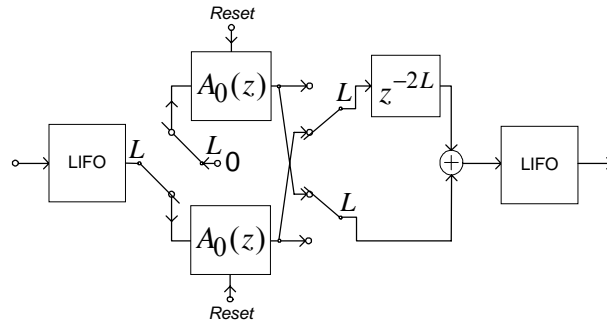

Fig. 2 – *Implementation block diagram of noncausal transfer function $A_0(z^{-1})$.*

5   Analysis of the Results

The design of an IIR QMF filter bank using two real allpass filters with $N = 4$, $\omega_p = 0.4\,\pi$ and $\omega_s = 0.6\pi$ is considered. The order of $H_0(z)$ is $2N + 1 = 9$, and the order of the allpass filters $A_0(z)$ and $A_1(z)$ is 2. Parameter K takes values $K = 1, 3, 5, 7, 9$ and, as $K = 2M + 1$, parameter M takes values $M = 0, 1, 2, 3, 4$. Value K is the number of zeros of the filter located at $z = -1$ and the order of the filter regularity.

The obtained magnitude responses of IIR half-band lowpass filters are shown in Figure 3. For $M = 4$ the design result is the Butterworth halfband filter and for $M = 0$ the result is the elliptic halfband filter. The Butterworth filter has a maximally flat magnitude response as it has 9 zeros at $z = -1$ and the highest possible regularity order, but it has the worst frequency selectivity. The lowest regularity order and the best selectivity the elliptic filter has. The halfband filters' poles are on the imaginary axis of the complex z plane and are complex-conjugated. All filter zeros are on the unit circle. The pole-zero plot of the IIR filter for $M = 0$ is shown in Figure 4. As $K = 1$ this filter has one zero at $z = -1$. Among the designed filters, the largest magnitude poles of the Butterworth filter are farthest from the unit circle, while the elliptic filter has poles nearest the unit circle.
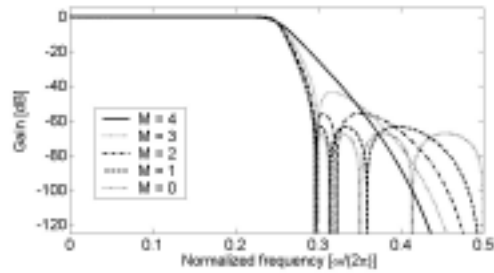
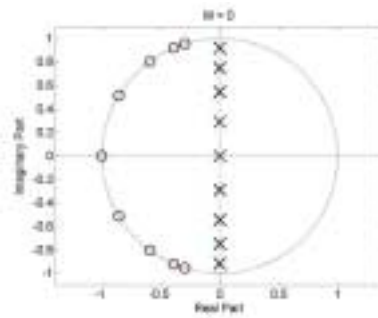**Fig. 3** – *Gain responses of IIR half-band lowpass filters.*

Fig. 4 – *Pole-zero plot of IIR half-band lowpass filter.*

The amplitude distortion functions and phase characteristics of filter banks for $M = 2$ and different block lengths are depicted in figures 5, 6 and 7. The amplitude distortion functions are close to 0 dB with a peak value, for $L = 20$ of 2.2 dB, for $L = 40$ of 0.1 dB and for $L = 60$ of $5 \cdot 10^{-3}$ dB. The phase responses are linear.
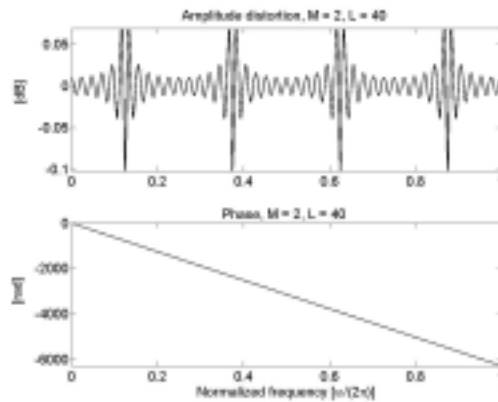

Fig. 5 – *Magnitude and phase response of IIR two-channel QMF bank for $L = 20$.*
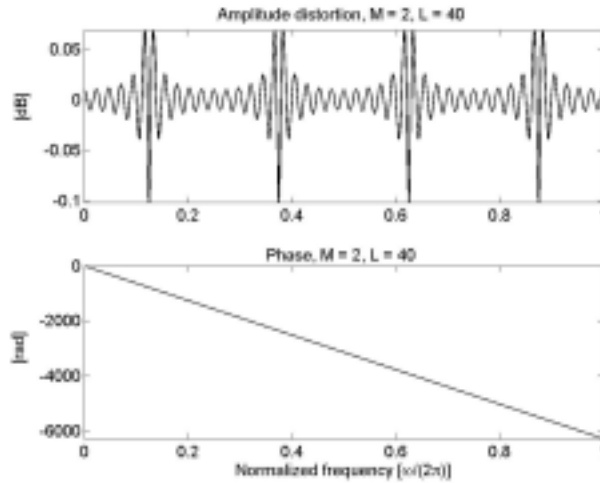
Fig. 6 - *Magnitude and phase response of IIR two-channel QMF bank for* $L = 40$.
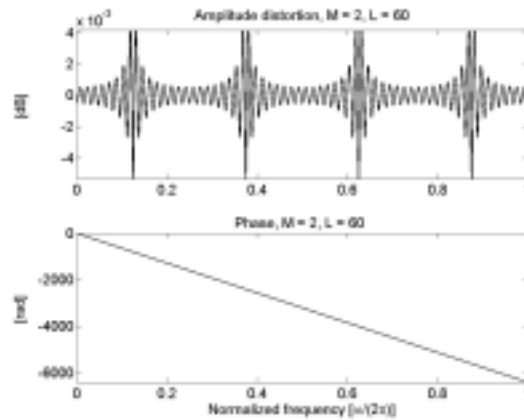

Fig. 7 - *Magnitude and phase response of IIR two-channel QMF bank for* $L = 60$.

Figure 8 shows the responses of designed filter banks when the input signal is a rectangular wave form and the length of the processing block amounts to $L = 20$. Figure 9 represents the magnified parts of the upper left corner of the rectangular wave form responses of the previous figure. It can be seen that the Butterworth filter response succeeds the shape of input signal very accurately, while the elliptic filter performs truncation of the rectangular corner. Figure 10 depicts the magnified upper edge or stationary part of the rectangular wave form responses, which are shown in Figure 8. The part of the Butterworth filter response best follows the input signal and has the smallest

deviations. As the M decreases, the block effect is more noticable. The elliptic filter has the greatest amplitude of distortion caused by the block processing. This is expected according to the position of poles which are nearest the unit circle.
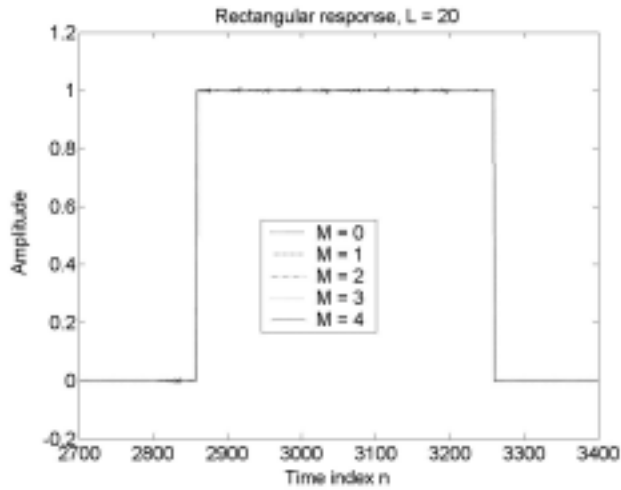

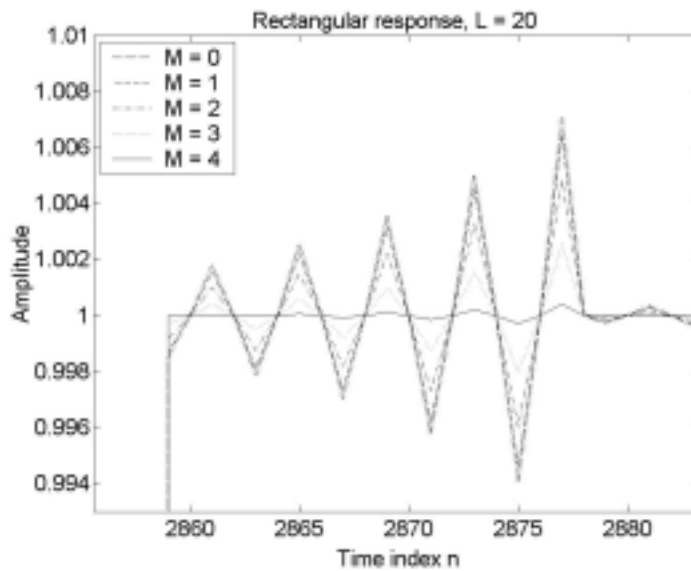**Fig. 8** – *Rectangular response of two-channel QMF bank.*

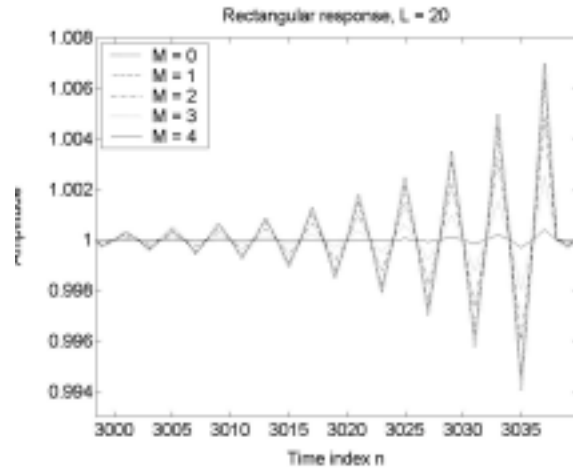**Fig. 9** – *Magnified response of the rectangular raising step, detail of Fig.6.*

Fig. 10 – *Magnified stationary part of the rectangular response, detail of Fig.6.*

Figure 11 depicts the influence of diferent block lengths on the distortion of the stationary part of the rectangular wave form responses. The block lengths of 20, 40 and 60 samples of the applied block processing technique are inspected. The block effect can be noticed as a periodical pattern sequence of $2L$ samples. The amplitude of distortion caused by the block processing is rapidly decreasing when the block length is increasing.
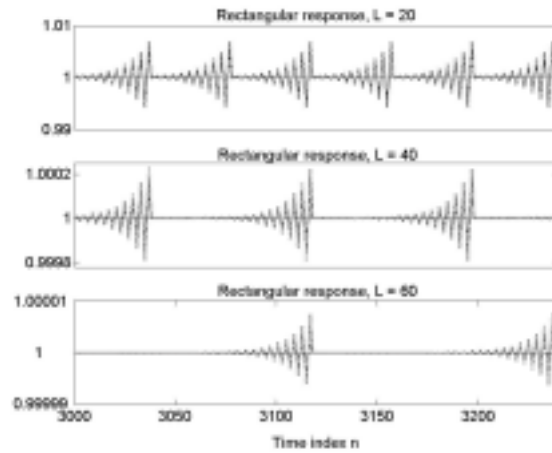

Fig. 11 – *Comparison of rectangular response stationary parts for different block lengths.*

Figure 12 shows the scaling and the wavelet functions generated according to [2] after five iterations of the analysis filter banks on the lowpass branch.
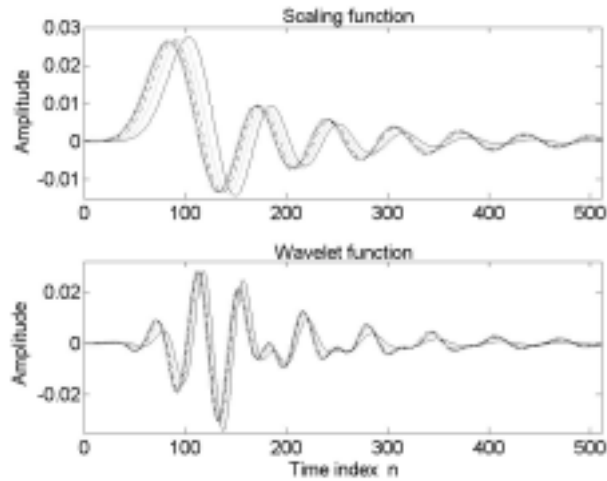
Fig. 12 – *Scaling and wavelet functions.*

6   Conclusion

In this paper, the implementation of two-band orthonormal IIR QMF filter banks using a parallel connection of two real allpass filters is examined. The criteria and the design algorithm of these IIR two-chanel filter banks are explained. The magnitude and phase characteristics of designed QMF banks are discussed according to filter poles position in the z-plane and the length of sequence used in block processing technique realization of anticausal filters. The generation of orthonormal wavelet bases by iterated designed orthonormal filter banks is presented.

7   References

[1] O. Rioul, P. Duhamel: A Remez Exchange Algorithm for Orthonormal Wavelets, IEEE Transactions on Circuits and Systems-II: Analog and Digital Signal Processing, Vol. 41, No. 8, pp. 550-560, August 1994.

[2] M. Vetterli, J. Kovačević: Wavelets and subband coding, New Jersey: Prentice Hall PTR, 1995.

[3] S. K. Mitra: Digital signal processing: a computer-based approach, Singapore: McGraw-Hill, 1998.

[4] C. Herley, M. Vetterli: Wavelets and recursive filter banks, IEEE Transactions on Signal Processing, Vol. 41, No. 8, pp. 2536-2555, August 1993.

[5] X. Zhang, T. Yoshikawa: Design of orthonormal IIR wavelet filter banks using allpass filters, Signal Processing, Vol. 78, Elsevier Science, pp. 91-100, 1999.

S. Damjanovi}, Lj. Mili}

[6] M. D. Lutovac, Lj. D. Milić: Approximate Linear Phase Multiplierless IIR Halfband Filter, IEEE Transactions on Signal Processing Letters, Vol. 7, No. 3, pp. 52-53, March 2000.

[7] Lj. Milić, M. Lutovac: Selective linear phase digital filters: theory and application, Facta universitatis (Niš), Series: Electronics and Energetics, Vol. 12, No. 2, pp. 187-207, 1999.